POURBAIX DIAGRAMS FOR IRON, NICKEL, AND CHROMIUM IN SUB-CRITICAL AND SUPERCRITICAL WATER

W.G. Cook and R. Olive

University of New Brunswick, Fredericton, New Brunswick, Canada

Abstract

The Supercritical Water-cooled Reactor presents many challenges in terms of material selection. Because the reactor will operate at temperatures and pressures above the critical point of water, an understanding of how candidate materials behave is essential. Pourbaix diagrams (a plot of electric potential vs. pH) are thermodynamic maps that predict the regions of immunity, passivity and reactivity of a particular metal in an aqueous environment. Pourbaix diagrams have been developed for the near-critical and supercritical regimes for iron, nickel, and chromium. Various sources were used for the necessary thermodynamic parameters, which were extrapolated to the temperatures of interest using the Helgeson-Kirkham-Flowers thermodynamic model and its revisions. The diagrams contain the ionic and aqueous species expected to be present under varying supercritical water density and temperature as well as the oxides expected to be formed under the given conditions for each of the individual metal-water systems.

1. Introduction

In the 21st century, the energy industry faces many formidable challenges. The general public is placing increasing importance on the environment and "green" technologies. As a result of this shift, companies and industries are being forced, in some cases, to alter longstanding ways of conducting business. The energy industry is no different. If current trends continue, "clean" energy sources that have no or low emissions of greenhouse gases will be favoured over their traditional, greenhouse gas emitting counterparts. Because of this, the future looks bright for nuclear power with its low emissions and its greater reliability as compared to both wind energy and solar power.

The supercritical water-cooled reactor (SCWR) is a Generation IV reactor concept that possesses several important advantages over nuclear reactors that are currently in operation. As the name implies, the SCWR uses supercritical water as the coolant, which provides higher thermodynamic efficiency due to the higher temperatures employed when compared to both its sub-critical light water and heavy water counterparts. The efficiency of the SCWR (~45%) will be greater than both the current LWRs and CANDU reactors (~33%) [1]. In addition, the commonly envisaged concept for the SCWR design is a direct cycle plant where there are no steam generators, resulting in a smaller reactor with lower capital costs. These advantages combine to make the SCWR an attractive option among the six selected Generation IV reactor technologies.

Several challenges must be overcome before the SCWR can be considered for construction. Because the SCWR operates above water's critical point, the materials used within the reactor must be able to withstand extremely high pressures and temperatures. Current conceptual designs are proposing pressures between 25 - 28 MPa and temperatures at the core outlet up to 625°C. Much work is currently underway to investigate the corrosion and degradation of candidate materials under these conditions. However, in addition to actual experimental testing, it is also useful to determine how these materials may behave from a theoretical basis. Pourbaix diagrams, plots of potential versus pH, are a thermodynamic map of the stability of metals, metal oxides and dissolved compounds at a given temperature, pressure and ionic concentration. These diagrams can provide insight into how a system behaves at various temperatures and pressures. Based on a detailed examination of Pourbaix diagrams for a particular metal system, optimum operating temperature and pressure can be selected theoretically on the basis of minimizing corrosion. This paper presents several Pourbaix diagrams of the iron-water, nickel-water, and chromium-water systems that have been constructed in the temperature and pressure ranges of interest for a SCWR and discusses the implications of using these metal-base alloys in a supercritical water environment.

The iron-water system is of particular significance because two groups of materials considered for the SCWR are the ferritic-martensitic (F/M) steels and the austenitic steels. F/M steels are an attractive candidate due to their resistance to irradiation induced cracking, low thermal expansion, and high thermal conductivity. Their oxides also have the advantage of being dense and resistant to spalling. However, F/M steels experience increasing oxide growth rates with increasing temperature above the critical point. This is problematic as the SCWR will use small wall thicknesses (0.63 mm for fuel cladding for example) and therefore thick oxide films must be avoided. In order for F/M steels to be utilized, the oxide growth rates must be mitigated. On the other hand, austenitic steels exhibit thinner oxide films but their oxides are very susceptible to spalling. While more experimental work is needed on both of these groups, it is useful to examine the thermodynamics of the iron-water system as a preliminary step [1].

Nickel-based alloys are also a potential option for SCWR construction. Ni-based materials exhibit the desirable trait of possessing high strength in high temperature applications. These alloys also exhibit low corrosion rates above the critical point. In addition, the oxide films that do form are very thin. However, Ni-based alloys have been shown to be quite susceptible to intergranular stress-corrosion cracking (IGSCC) in supercritical water, especially when compared to the F/M steels [1]. Nickel alloys also may be susceptible to helium embrittlment if they are used as a material of construction in the core of the reactor since an alpha-particle (He nucleus) is emitted when nickel absorbs a neutron, which can accumulate at defects or in voids in the metal lattice.

Chromium is an important alloying element in many alloys as it provides corrosion resistance. The oxide chromite, Cr_2O_3, serves as a passivating layer when chromium is alloyed in various metals including iron and nickel. Therefore, the chromium-water system is of interest to SCWR research. However, before materials with chromium as alloying metal can be considered for supercritical applications, the stability limit of chromite in terms of temperature and pressure and potential oxidising conditions must be determined.

2. Calculation methods

Pourbaix Diagrams (E vs pH diagrams) are constructed using the Nernst Equation that describes the equilibrium potential of a given electrochemical reaction as a function of the proposed reaction's standard potential, the system's pH, temperature and the activity (concentration) of the dissolved species. The standard potential of a reaction at a given temperature may be easily evaluated through the Free Energy change. Therefore, it is necessary to determine the Gibbs Free Energy of formation for each species involved in the given reaction at the temperatures and pressures of interest. Tabulated values of the Gibbs Free Energy of formation are typically presented at the reference temperature of 25°C, so a calculation must be made to extrapolate these known values to the temperature and pressure of interest. This is a relatively simple procedure for pure compounds (solids, liquids, gases) where the temperature dependence of the specific heat capacity is know accurately over a wide temperature range. For these substances, we can use the basic relation:

$$G^o_{(T_2)} = G^o_{(T_1)} - S^o_{(T_1)}\left[T_2 - T_1\right] - T_2\int_{T_1}^{T_2} \frac{C^o_p}{T}\,dT + \int_{T_1}^{T_2} C^o_p\,dT \tag{1}$$

where $G^o{}_{(T2)}$ is the Gibbs Free Energy at the temperature of interest (T_2), $G^o{}_{(T1)}$ is the Gibbs Free Energy under reference conditions (T_1 = 298 K); $S^o{}_{(T1)}$ – standard molar entropy under reference conditions; $C_p{}^o$ – isobaric molar heat capacity (a temperature dependent parameter typically described by a polynomial fit to experimental data).

The extrapolation procedure is much more complex for dissolved aqueous species and ions in solution since heat capacity of a solute does not particularly have any meaning and is typically not know as a function of temperature, if at all. Thus, alternate calculation methods are required and involve extrapolations using known standard state thermodynamic properties and solute or ion specific "fit" parameters that are determined experimentally. The semi-empirical revised Helgeson-Kirkham-Flowers (R-HKF) model is employed in this work.

For the R-HKF model, the Gibbs free energy of formation of a solute molecule (ion or aqueous species) is defined as the sum of the standard Free Energy under reference conditions and the Free Energies of solvation and non-solvation, which are highly dependent on the temperature and pressure:

$$\Delta G^o_i = \Delta G^o_{r,i} + \Delta G^o_{s,i} + \Delta G^o_{n,i} \tag{2}$$

where $\Delta G^o{}_i$ is the Gibbs free energy of species i at the specified temperature and pressure, $\Delta G^o{}_{r,i}$ is the Gibbs Free Energy of formation of species i at reference conditions (0.101325 MPa and 298 K), $\Delta G^o{}_{s,i}$ is the solvation Gibbs free energy change for species i, and $\Delta G^o{}_{n,i}$ is the nonsolvation Gibbs free energy change for species i. The solvation and non-solvation parameters are complex functions of temperature and pressure as well as the standard state specific molar entropy, specific molar heat capacity and specific molar volume (for more details see references 7 – 10).

Several sources were used to obtain the Gibbs Free Energy of formation and other thermodynamic parameters at reference conditions. For the ionic species Fe^{2+}, Fe^{3+}, Ni^{2+}, Cr^{2+}, and Cr^{3+}, values were taken from Shock et al. [2], where thermodynamic values for Ni_3O_4, Ni_2O_3, NiO_2, CrO_2^-, and CrO are from Roberge [3]. All other data for the remaining species are from Beverskog and Puigdomenech [4, 5, 6]. It must be pointed out that the calculated high-temperature Free Energy of each ion is only as accurate as the fit parameters in the HKF model allow and should be validated with high-temperature thermochemical data – much of which is currently unavailable or is of low certainty. However, as a first trial at composing the high temperature diagrams, the data sources shown above are sufficient. Validation of the parameters used in the HKF model, such as providing a self-consistent database of the HKF parameters from the most reliable high temperature measurements of oxide solubility (for example Tremaine and Leblanc [11]) as described in reference 12 will be undertaken in the future.

Calculations were performed using the standard techniques and the R-HKF model to extrapolate the thermodynamic data to the temperatures and pressures of interest using the equations and approximations given in several sources [7,8,9,10]. In addition, an approximation by Sue et al. was employed in order to give a validated extrapolation up to 600^{o}C, 998 bar, and to a minimum water density of 0.2 g/cc [13].

3. Results and Discussion

Pourbaix diagrams were constructed for iron, nickel, and chromium at 25 MPa. Two diagrams for each metal-water system are presented: one slightly below the pseudo-critical point and one slightly above (diagrams at higher temperatures were also constructed but differed very little from the diagram presented just above the critical point). All diagrams presented were constructed at a dissolved ion concentration of 10^{-8} molal as this is thought to be representative of the dissolved species concentration in high-temperature water (however, for supercritical water the concentration is expected to be several orders of magnitude lower). The dashed vertical line denotes the neutral pH of water at the temperature and pressure in question. This is of particular interest to the SCWR design since most chemistry conditions evaluated to date have used pure, deoxygenated water; thus, the dashed vertical line on each diagram represents the potential “operating” pH value for the SCWR with pure neutral water. The dashed sloping lines enclose the area where water is stable. The upper line denotes the equilibrium of the oxygen reduction reaction whereas the lower line represents the equilibrium for hydrogen evolution.

3.1 The iron-water system

Figure 1 shows the Pourbaix diagram for the iron-water system at 10 MPa and 300^{o}C, which was used for validation against the diagrams described by Beverskog and Puigdomenech [4]. With the exception that the diagram presented here omits the $Fe(OH)_{3(aq)}$ region because the $Fe_2O_3/Fe(OH)_3$ equilibrium is independent of both potential and pH, the diagrams agree quite well.

Figure 2 shows the Pourbaix diagram for the iron-water system at 25 MPa and 350°C, conditions that are below the critical temperature. As at the lower temperature shown in Figure 1, under these conditions, two passive areas are formed: Fe_3O_4 (magnetite) and Fe_2O_3 (hematite). The immunity region for iron is located below the hydrogen evolution line. It should also be noted that, in sub-critical conditions, the aqueous species $Fe(OH)_2$ separates the immunity region from the passive region and is bisected by the hydrogen evolution line. This implies that, in completely deoxygenated high temperature water where hydrogen evolution is the only reduction couple possible, iron-based steels would be in a regime of active corrosion.

Figure 3 shows the iron-water system at 400°C and 25 MPa, conditions that are above the pseudo-critical point (~ 385°C at 25 MPa). In this diagram, the regions of corrosion have been greatly reduced. The predominance regions of magnetite and hematite have grown significantly and no area of corrosion exists at high pH values. Under more acidic conditions and as the electrochemical potential becomes more oxidizing, aqueous ferrous and ferric species are stable. In the neutral pH region where a SCWR is expected to operate, only passive oxides (magnetite and heamatite) are stable at 10^{-8} mol/kg. It is interesting to note that, since the solubility of iron in water is expected to drop by several orders of magnitude upon passing the critical point, the concentration of 10^{-8} mol/kg severely overestimates the iron concentration at the metal/solution interface. Predictions can be made of the approximate range of the solubility of iron in SCW by lowering the concentration and observing when the "soluble" species appear. Figure 4 shows the Pourbaix diagram for iron-water at 400°C, 25 MPa and 10^{-12} mol/kg. It is apparent that only soluble species are stable at this lower concentration. When 10^{-11} mol/kg is chosen, the diagram is almost identical to Figure 3. From this, we can assume the solubility of iron in SCW at 400°C and 25 MPa is between 10^{-12} – 10^{-11} mol/kg.

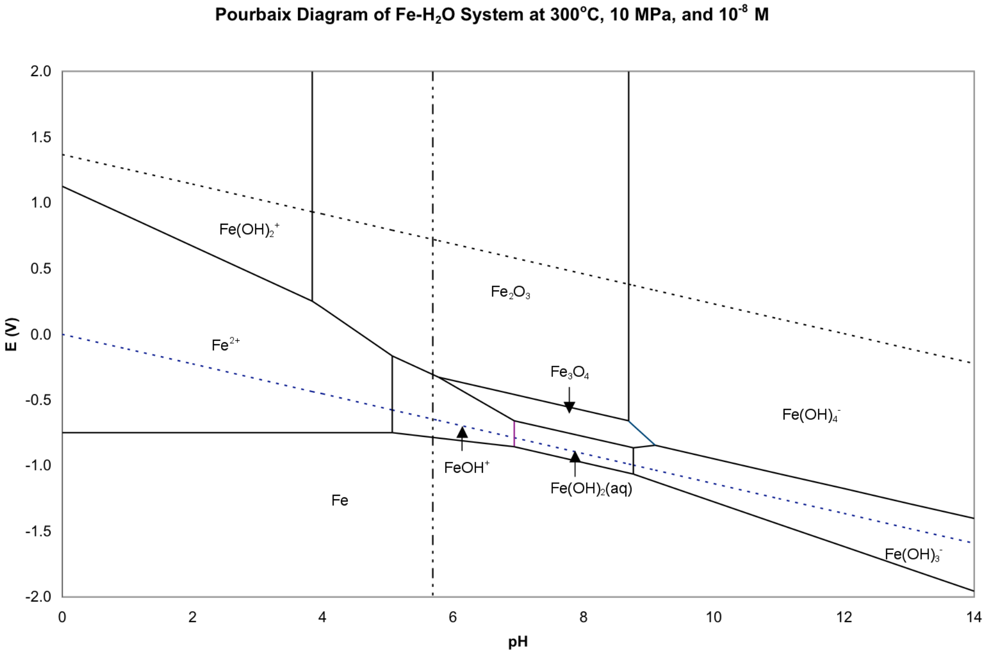

Figure 1. Pourbaix diagram of the Fe-H_2O system at 300°C, 10 MPa, and 10^{-8} molal.

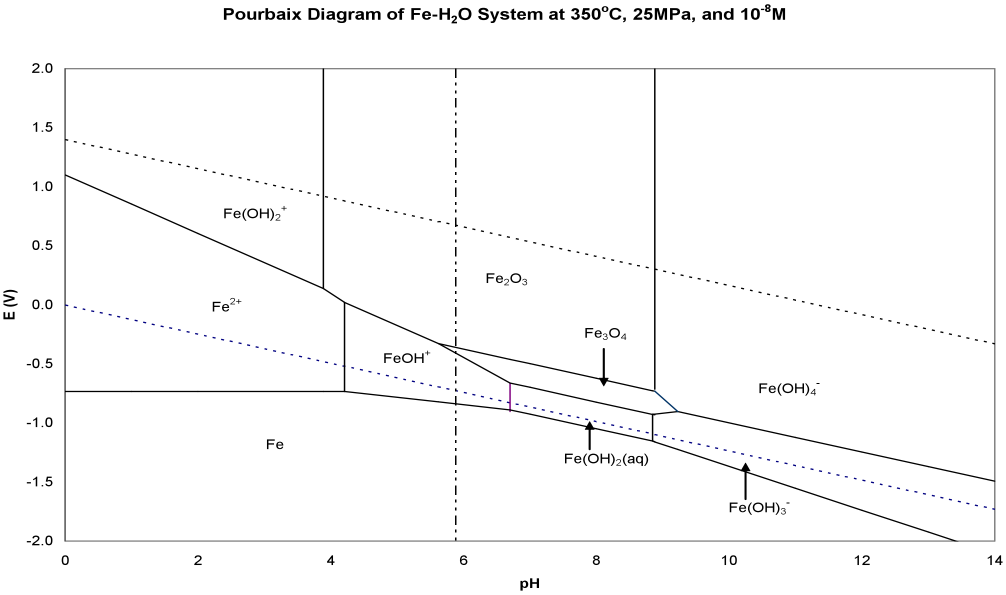

Figure 2. Pourbaix diagram of the Fe-H_2O system at 350°C, 25 MPa, and 10^{-8} molal.

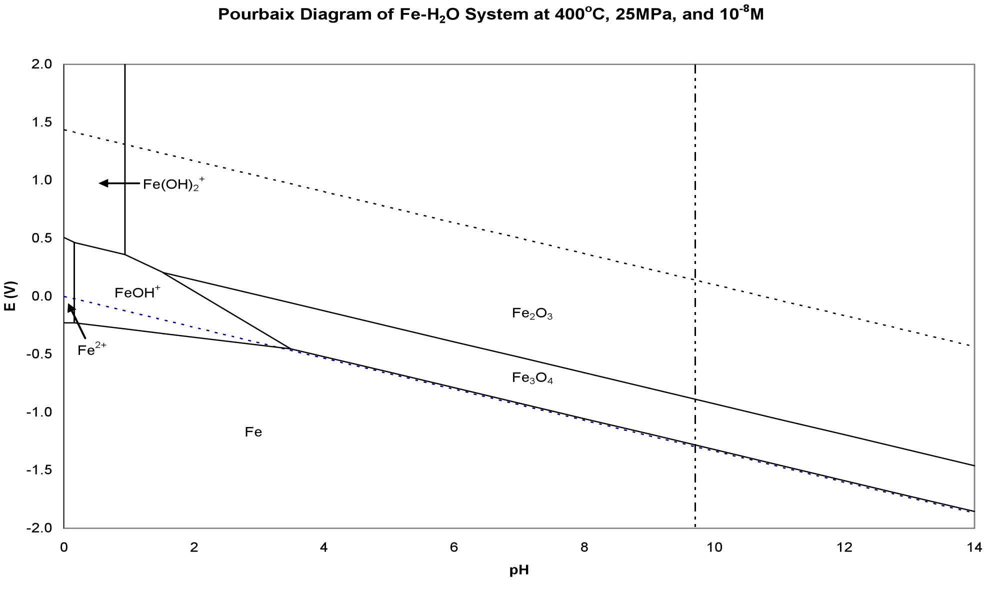

Figure 3. Pourbaix diagram of the Fe-H_2O system at 400°C, 25 MPa, and 10^{-8} molal.

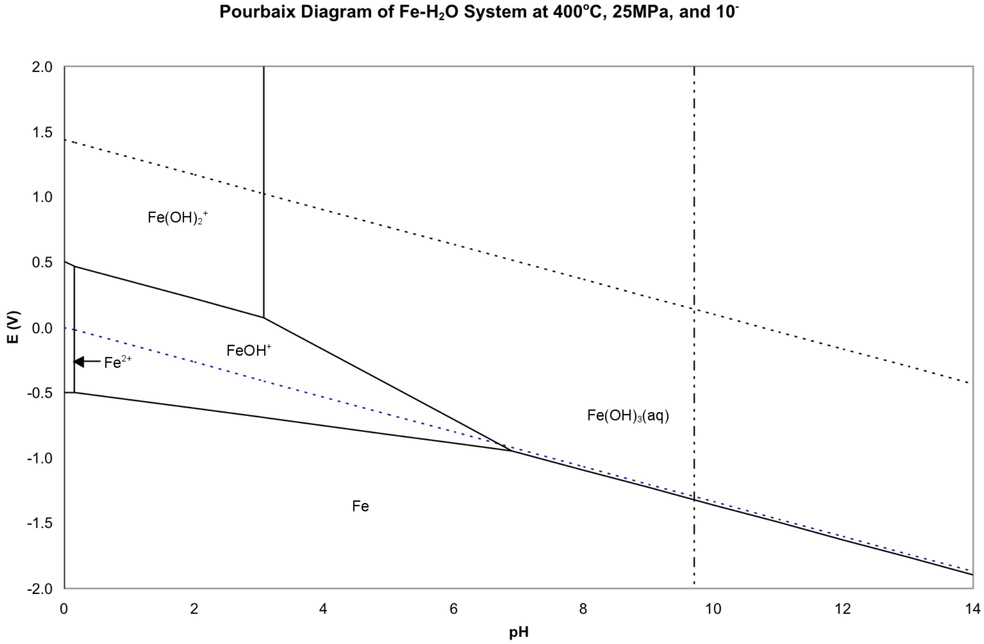

Figure 4. Pourbaix diagram of the Fe-H_2O system at 400°C, 25 MPa, and 10^{-12} molal.

3.2 The nickel-water system

Figure 5 shows the Pourbaix diagram for the nickel-water system at 25 MPa and 350°C. Nickel exhibits a large area of immunity at 350°C and, under the neutral water conditions proposed for a SCWR, should be immune to oxidation under reducing conditions since the Ni/NiO transition is well above the hydrogen evolution line. In fact, below the critical temperature nickel only exhibits stable passive oxides (NiO, Ni_3O_4, Ni_2O_3 and NiO_2) under neutral conditions. Under acidic and alkaline conditions, the Ni^{2+} and $Ni(OH)_3^-$ corrosion areas are prevalent respectively. If oxidising conditions are present, for example due to radiolysis products produced in a sub-critical section of a SCWR, nickel-based alloys could form several different oxide phases, NiO or Ni_2O_3. Like in conventional reactors, it is known that nickel-based alloys are susceptible to stress corrosion cracking, particularly under oxidising conditions, which may be partially due to stresses induced through phase transitions between the metal and these passive films.

Figure 6 shows the nickel Pourbaix diagram for 25 MPa and 400°C, conditions above the pseudo-critical point. Like the iron-water system, passive films predominate under neutral conditions. At 10^{-8} mol/kg, the only aqueous predominance area is Ni^{2+} which exists under very acidic conditions and potentials above the hydrogen evolution reaction. The rest of the diagram consists of regions of passivity belonging to several oxides of nickel including NiO, Ni_3O_4, Ni_2O_3 and NiO_2. Depending upon the oxygen content (p_{O2}) in the SCW circuit, any of the oxides could form, which could promote SCC of nickel-based alloys, as in sub-critical water.

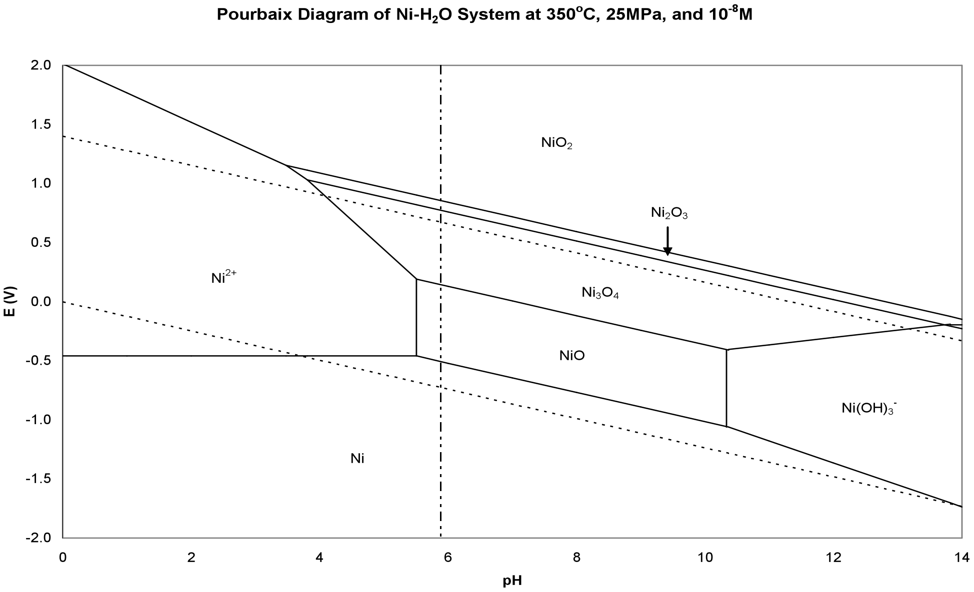

Figure 5. Pourbaix diagram of the Ni-H$_2$O system at 350°C, 25 MPa, and 10^{-8} molal.

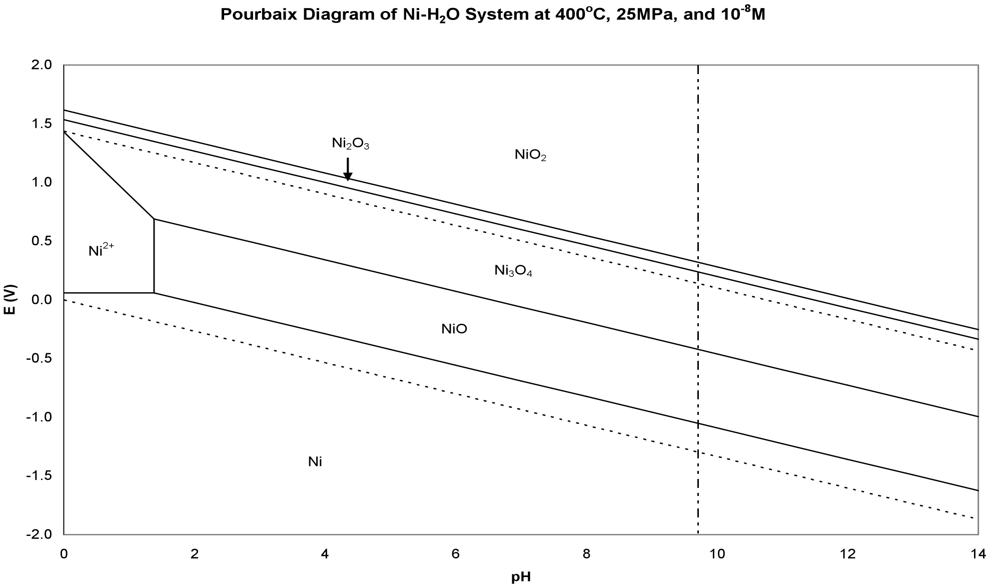

Figure 6. Pourbaix diagram of the Ni-H$_2$O system at 400°C, 25 MPa, and 10^{-8} molal.

3.3 Chromium-water system

Figure 7 shows the Pourbaix diagram for the chromium-water system at 350°C and 25 MPa. There is only one area of passivity in the diagram, which is the large predominance area of chromite, Cr_2O_3. Under strongly acidic or alkaline conditions, no stable solid phase of chromium is shown to exist and, as expected, the chromite is shown to be unstable under oxidising conditions where the soluble species H_2CrO_4, $HCrO_4^-$ and CrO_4^{2-} are shown to be the stable phases. As in any nuclear heat transport system where a steel's corrosion protection relies upon the formation of a chromite oxide film, it will be necessary to strictly control the oxidising nature of the reactor coolant to prevent dissolution and transport of soluble chromium species.

Above the critical point, a second passivity region appears in the form of CrO. As can be seen in Figure 8, large passive regions for CrO and Cr_2O_3 exist over very large pH range. There also exists a small corrosion region in very acidic conditions for Cr^{2+}. As in the sub-critical case described above, as the potential becomes more oxidizing, the aqueous H_2CrO_4 species becomes the stable phase. The appearance of the second oxide phase under supercritical conditions is interesting. If both CrO and Cr_2O_3 oxides can be formed, the transition from one phase to the next could induce considerable stresses on the surfaces of the materials and could act as potential initiation for a stress-corrosion crack, analogous to oxide phase transitions in the nickel-based alloys in sub-critical and supercritical conditions. As a result, control of oxidising conditions in the reactor coolant will be essential for any metal relying on the establishment of chromite as its passive film for corrosion protection and the presence of multiple chromium oxides (and nickel oxides for that matter) may be at least partially responsible for the increased SCC susceptibility under supercritical water conditions.

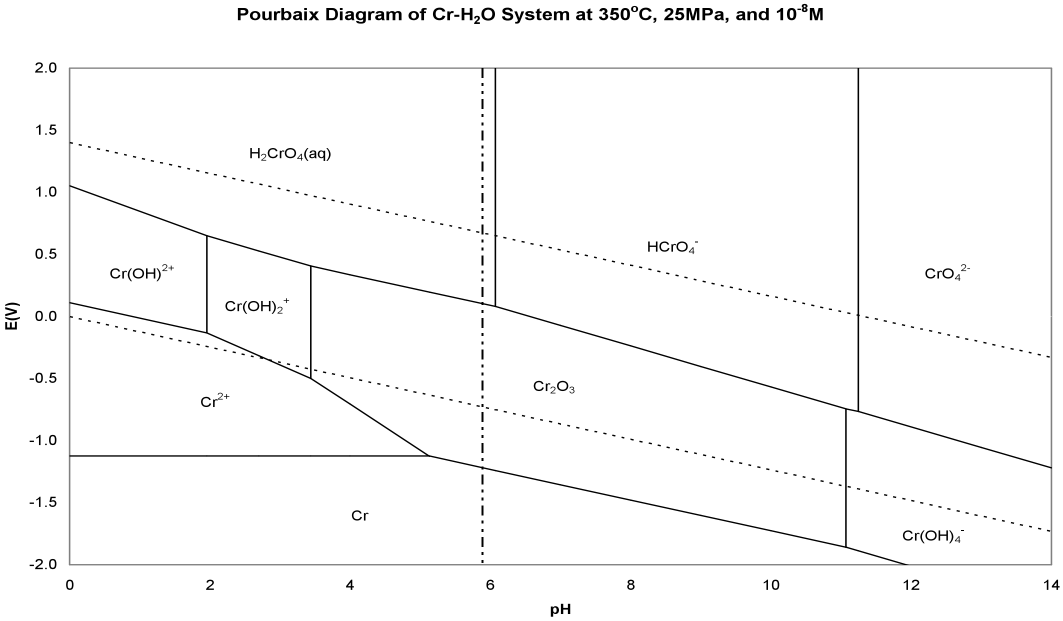

Figure 7. Pourbaix diagram of the Cr-H_2O system at 350°C, 25MPa, and 10^{-8} molal.

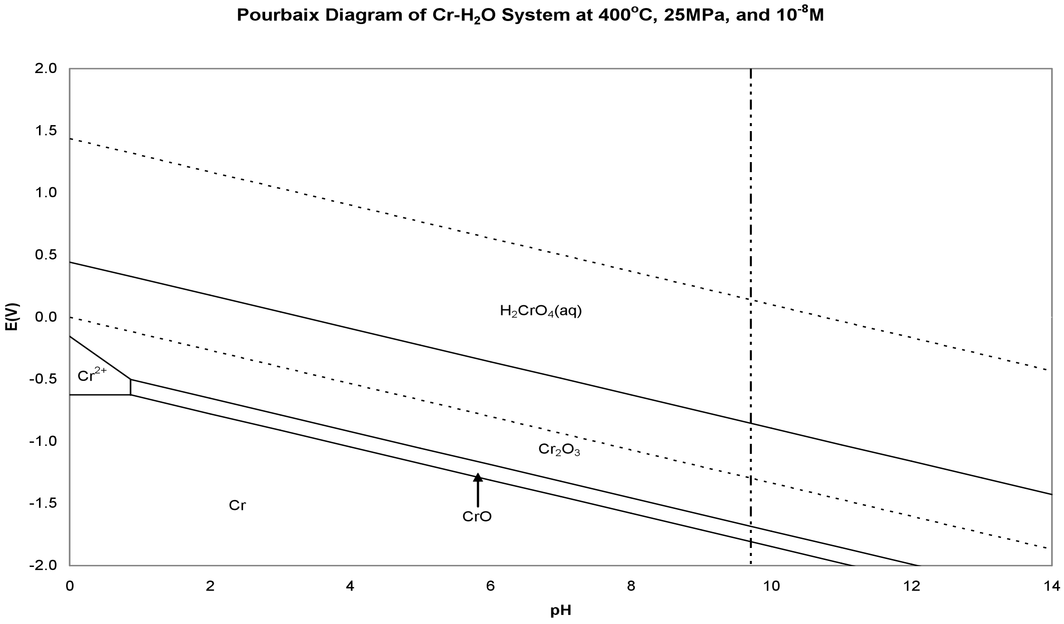

Figure 8. Pourbaix diagram of the Cr-H_2O system at 400°C, 25MPa, and 10^{-8} molar.

4. Conclusions

Several Pourbaix diagrams have been presented for the iron-water, nickel-water, and chromium-water systems at both subcritical and supercritical conditions. All systems undergo dramatic changes as the critical point is passed. Iron displays regions of immunity and passivity at mid- to high-pH values regardless of potential. However, in subcritical conditions with temperatures approaching the critical point, the immunity region is separated from the passivity areas by corrosion regions, particulary the ferrous hydroxides $Fe(OH)^+$, $Fe(OH)_{2(aq)}$ and $Fe(OH)_3^-$. Nickel is quite stable in supercritical conditions with only a small corrosion area in extremely acidic conditions. In subcritical conditions, the nickel shows passivation regions in the neutral pH range. As expected, chromium shows large passive regions due to the formation of chromite in sub-critical conditions and a combination of chromium oxide and chromite under supercritical conditions. Chromium is seen to exhibit corrosion regions based upon $H_2CrO_{4(aq)}$, $HCr_2O_4^-$ and $Cr_2O_4^{2-}$ as the potential becomes oxidizing and pH increases in both sub- and supercritical conditions, with $H_2CrO_{4(aq)}$ being the sole species present above the critical point. Based on these diagrams, it is apparent that any steels or alloys that depend upon chromite for corrosion protection are to be used carefully and in reducing conditions.

5. Acknowledgements

The authors thank the Natural Science and Engineering Research Council (NSERC) for the funding to carry out this work.

6. References

[1] G.S. Was et al., "Corrosion and stress corrosion cracking in supercritical water", *Journal of Nuclear Materials*, Vol. 371, 2007, pp.176-201.

[2] E. L. Shock et al., "Inorganic species in geologic fluids: Correlations among standard molal thermodynamic properties of aqueous ions and hydroxide complexes", *Geochimica et Cosmochimica Acta*, Vol. 61, 1997, pp.907-950.

[3] P. R. Roberge, *Handbook of Corrosion Engineering*, McGraw-Hill, 2000.

[4] B. Beverskog and I. Puigdomenech, "Revised Pourbaix diagrams for iron at 25-300°C", *Corrosion Science*, Vol. 38, 1996, pp.2121-2135.

[5] B. Beverskog and I. Puigdomenech, "Revised Pourbaix diagrams for nickel at 25-300°C", *Corrosion Science*, Vol. 39, 1997, pp.969-980.

[6] B. Beverskog and I. Puigdomenech, "Revised Pourbaix diagrams for chromium at 25-300°C", *Corrosion Science*, Vol. 39, 1997, pp.43-57.

[7] N. Saito et al., "Chemical thermodynamics consideration on corrosion products in supercritical-water-cooled reactor coolant", *Nuclear Technology*, Vol. 155, 2006, pp.105-113.

[8] E. L. Shock and H. C. Helgeson, "Calculation of the thermodynamic and transport properties of aqueous species at high pressures and temperatures: Correlation algorithms for ionic species and equation of state predictions to 5kb and 1000°C", *Geochimica et Cosmochimica Acta*, Vol. 52, 1988, pp.2009-2036.

[9] E. L. Shock, "Calculation of the thermodynamic and transport properties of aqueous species at high pressures and temperatures: effective electrostatic radii, dissociation constants and the standard molal properties to 1000°C and 5 kbar", *J. Chem. Soc., Faraday Trans.*, Vol. 88, 1992, pp.803-826.

[10] E. H. Oelkers et al., "Summary of the apparent standard partial molal Gibbs free energies of formation of aqueous species, minerals, and gases at pressures 1 to 5000 bars and temperatures 25 to 1000°C", *J. Phys. Chem. Ref. Data*, Vol. 24, 1995, pp.1401-1560.

[11] P.R. Tremaine and J.C. LeBlanc, "The solubility of magnetite and the hydrolysis and oxidation of Fe^{2+} in water to 300°C", *J. Sol. Chem.,* vol.9, 1980, pp.415

[12] F. Brosseau, D. Guzonas and P. Tremaine, "Predicting iron transport in a supercritical water cooled pressure tube reactor", *Proceedings of the 30th Annual Conference of the Canadian Nuclear Society*, Calgary, 2009.

[13] K. Sue et al., "Predictive model for equilibrium constants of aqueous inorganic species at subcritical and supercritical conditions", *Ind. Eng. Chem. Res.*, Vol. 41, 3298, pp.3298-3306.